Lifetimes of $n\,^2P$ states of thallium by analysis of cascade fluorescence following two-photon excitation

John V. James and Charles C. Wang
Research Staff, Ford Motor Company, Dearborn, Michigan 48121

Curtis Doty
Department of Electrical Engineering, Wayne State University, Detroit, Michigan 48202

(Received 3 February 1986)

The lifetimes of the $n\,^2P_{1/2}$ and $n\,^2P_{3/2}$ states of thallium, $n=7-11$, have been determined through measurements of the fluorescence signal resulting from two-photon excitation in an atomic beam. The temporal dependence of the fluorescence signal is determined by solving the equations governing cascade spontaneous fluorescence from higher-lying initial states. It is shown that under conditions applicable to our experiments, the asymptotic decay of the fluorescence is a measure of the lifetime of the initial state. The possibility of self-absorption of the fluorescence within the atomic beam is investigated; it is found to be negligible over the range of thallium densities used in the experiment. Our lifetime measurements for these eight ^2P states are compared with other known experimental data and with the results of previous semiempirical calculations.

I. INTRODUCTION

Lifetime measurements by observation of spontaneous fluorescence following two-photon excitation have been previously reported[1] for the $7\,^2P_{1/2}$ and $7\,^2P_{3/2}$ states of thallium. The results not only demonstrated the usefulness of this technique for measuring lifetimes of states having the same parity as the ground state, but they also provided an important comparison with various semiempirical calculations[2–4] which have been performed for oscillator strengths of thallium. This comparison is extended in the present work, which reports lifetimes of the $n\,^2P_{1/2}$ and $n\,^2P_{3/2}$ states of thallium for $n=8-11$, as well as repeated measurements of the $7\,^2P$ states. In addition, we include lifetime values for the $7\,^2P_{1/2}$, $7\,^2P_{3/2}$, and $8\,^2P_{3/2}$ states obtained earlier by Hunter, Commins, and Roesch[5] from their Hanle-effect measurements.[6]

The semiempirical calculations mentioned above all employ a one-electron central-field model for the atom, because thallium has only a single valence electron beyond completely filled subshells. Although this treatment ignores configuration mixing, the agreement with experimental oscillator strengths and lifetimes is quite good in some cases. The calculations of Bardsley and Norcross[3] are perhaps the most accurate; their inclusion of core-polarization effects yields results which agree very well with available data. However, the scarcity of experimental values involving the ^2P states of thallium was the impetus for our initial measurements of the lifetimes of the $7\,^2P$ states; this paper significantly enhances this comparison by extending the lifetime measurements of the excited $n\,^2P$ states to $n=11$.

The essential features of the experiment remain unchanged from our previous description, which is reviewed briefly in Sec. II. However, for the higher-lying $n\,^2P$ states excited in the present experiments, the cascade fluorescence spectrum is much more complicated than before. This point can be appreciated by considering the energy-level diagram of thallium[7] shown in Fig. 1. For a $7\,^2P$ initial state, all radiative decay occurs via the $7\,^2S_{1/2}$ state to one of the $6\,^2P$ states; for higher-lying initial $n\,^2P$ states, the possible decay paths rapidly become more numerous as the value of n increases. This myriad of de-

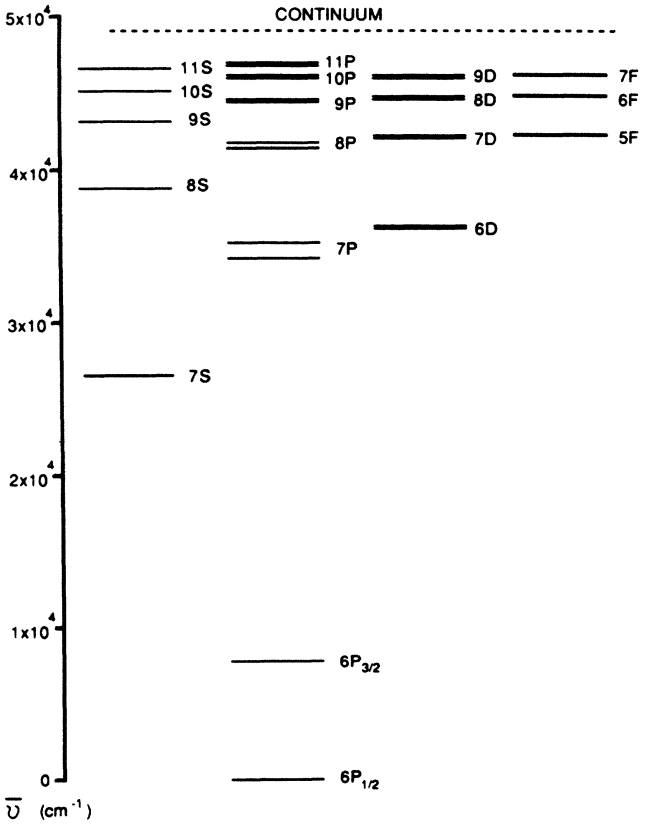

FIG. 1. Energy-level diagram of thallium.

cay paths means that the time evolution of the cascade fluorescence is a function of the lifetimes of the lower-lying states as well as the lifetime of the initial state. Fortunately, the conditions of our experiments are such that the asymptotic behavior of the fluorescence decay is determined solely by the lifetime of the initial state, even for light emitted by lower-lying states. This is the subject of Sec. III, which also includes computer simulations of the spontaneous radiative decay of an atom in a single initial excited state. Section IV discusses the errors (both systematic and statistical) which pertain to this experiment, including a brief investigation into possible self-absorption of the fluorescence within the atomic beam. Section V summarizes the lifetime results and compares them with theoretical and other experimental values.

II. EXPERIMENTAL PROCEDURE

Lifetime measurements reported in this paper were carried out using the same technique as described previously,[1] with some exceptions to be noted. Thallium atoms in an atomic beam are excited to an $n\,^2P$ state through two-photon absorption of light from the output of a tunable pulsed dye laser. The cascade fluorescence which results from spontaneous decay of this and lower-lying states is sampled by a photomultiplier tube (PMT), and recorded as a function of time following each laser pulse. The lifetime of the initial state is deduced from the fluorescence signal.

In the previous experiments, the fluorescence signal was recorded with a Princeton Applied Research analog boxcar. This has been replaced with a Data Precision 6000 series waveform digitizer-averager instrument, which samples 64 points per waveform at intervals of 10—40 ns, depending on the transition. The main advantage of this instrument is that the entire fluorescence-decay curve is digitized for each laser shot, thus allowing the average signal to be acquired much more rapidly than with the analog instrument. (The analog boxcar sweeps a single gate across the decay curve in *successive* shots of the laser, thus wasting the major portion of the fluorescence signal.) This also eliminates the possibility that drift in system parameters during averaging will appear as deviations from the exponential decay.

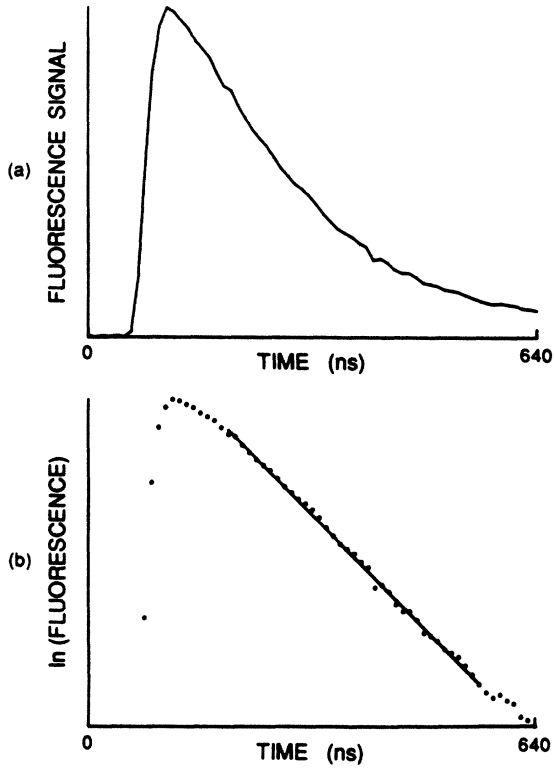

FIG. 2. Fluorescence signal resulting from the $8\,^2P_{1/2}$ initial state. (a) Fluorescence decay vs time. (b) Lifetime determined by the least-squares fit of the logarithm of the data to a straight line over the indicated range.

The improved acquisition method was necessitated in part by the lower signal levels encountered in measurements of the $n\,^2P$ for $n \geq 8$ compared to the $n=7$ case. At least part of this is due to the smaller laser energies obtainable with the dyes used in the $n \geq 8$ experiments. Table I shows the wavelength needed to reach each state, along with the dye used and the pump wavelength. Only the $n=7$ case utilizes pumping by the second harmonic of the Nd:YAG laser (YAG denotes yttrium-aluminum-garnet); all others use the much weaker third-harmonic

TABLE I. Laser parameters for the transitions studied. The wavelength of the dye laser is chosen to populate the initial state by two-photon excitation.

Excited state	Dye laser λ (nm)	Laser dye used	Typical energy (mJ)	Pump λ (nm)
$7\,^2P_{1/2}$	585.5	Kiton red 620	9.0	532
$7\,^2P_{3/2}$	568.8	Rhodamine 590	12.0	532
$8\,^2P_{1/2}$	483.5	LD 490	0.8	355
$8\,^2P_{3/2}$	479.2	LD 490	1.3	355
$9\,^2P_{1/2}$	450.6	Coumarin 445	1.0	355
$9\,^2P_{3/2}$	448.8	Coumarin 445	1.0	355
$10\,^2P_{1/2}$	435.4	Coumarin 440	1.0	355
$10\,^2P_{3/2}$	434.4	Coumarin 440	1.0	355
$11\,^2P_{1/2}$	426.9	Stilbene 420	1.3	355
$11\,^2P_{3/2}$	426.3	Stilbene 420	1.3	355

beam as a pump. For these measurements, the dye-laser system is a conventional pulsed oscillator followed by a pulsed-amplifier stage.

Figure 2 shows a typical fluorescence signal obtained with the waveform digitizer after averaging for 2000 laser shots, or about 3 min acquisition time. Figure 2(a) is the time decay of cascade fluorescence resulting from the $8\,^2P_{1/2}$ initial excited state. For the lower-lying states ($7\,^2P_{1/2,3/2}$), the fluorescence at 378 nm from the $7\,^2S_{1/2}-6\,^2P_{1/2}$ transition is monitored; for $n=8$ and above, this line is excluded from detection by placing a cell containing an aqueous solution of $NiSO_4$ in front of the PMT. The choice of which wavelengths to include in the fluorescence detection is discussed in Sec. III.

III. ANALYSIS OF CASCADE FLUORESCENCE

The analysis of the data is essentially very straightforward—plot the logarithm of the fluorescence signal and then fit the points to a straight line to determine the lifetime of the initial state. An example of this is shown in Fig. 2(b) for the $8\,^2P_{1/2}$ state. However, because the detected fluorescence consists of lines originating from lower-lying states that are populated by decay from the initial excited state, some conditions must be met before the slope as deduced above can be related directly to the lifetime of the initial excited state. These conditions can be understood by considering the time evolution of the population distribution among the various states following excitation.

When the lifetime of the initially populated state is much longer than the duration of the laser beam, the details of the excitation process can be replaced by a simple approximation. At $t=0$, the atom can be assumed to be in one particular excited state (label N), from which it decays according to the rate equation

$$\dot{\mathbf{n}}(t)=\underline{A}\,\mathbf{n}(t)\ , \tag{1}$$

where $\mathbf{n}(t)$ is the vector representing the population distribution in the various levels at time t after the laser pulse, and $\underline{A}$ is the rate matrix for spontaneous decay between levels. Because only downward transitions can occur in spontaneous decay, $\underline{A}$ is subject to the following restrictions:

$$A_{ij}\begin{cases}=0, & i>j\\ <0, & i=j\\ >0, & i<j,\end{cases} \tag{2}$$

where A_{ij} is the spontaneous radiative transition rate from level j to level i. Note that this formulation assumes that $E_j>E_i$ if $j>i$. Furthermore, the total population in all the states is constant (equal to the initial value, which is chosen as one in this normalization). This constraint leads to

$$\sum_i A_{ij}=0,\quad \text{for all } j\ . \tag{3}$$

A characteristic of this system is that if the initial state N has a lifetime τ_N which is longer than that of any other state emitting fluorescence, then the fluorescence decay from any state will asymptotically approach a single exponential which is determined solely by the lifetime of the initial state and does not depend on the lifetime of the state emitting the fluorescence. This follows from an examination of the solution to Eq. (1). In general, the time evolution of the population distribution is given by

$$\mathbf{n}(t)=\sum_j c_j\mathbf{n}^j e^{-t/\tau_j}\ , \tag{4}$$

where the c_j are determined by the initial conditions and the $\mathbf{n}^j$ are eigenvectors satisfying the eigenvalue equation

$$\underline{A}\,\mathbf{n}^j=-\lambda_j\mathbf{n}^j\ . \tag{5}$$

Because $\underline{A}$ is an upper-diagonal matrix, the eigenvalues λ_j are just the inverses of the lifetimes τ_j of the states of the system. Also, the initial condition gives $c_j=0$ for all states j above the initial state. Thus, since all fluorescent components are of the form $A_{ik}n_k(t)$, the asymptotic limit of all spectral lines behaves as e^{-t/τ_N}, as long as τ_N is the largest of all pertinent lifetimes. (Ground or metastable states are excepted since they do not contribute to the fluorescence.)

Of course, how rapidly the signal approaches the asymptotic limit depends on the actual solution indicated by Eq. (4), as well as the relative sensitivity of the fluorescence detector to each of the spectral lines emitted. Obviously, the additional exponential terms indicated in Eq. (4) will decay more quickly if the lower states have much shorter lifetimes than the initial state. However, a quantitative determination of their contribution as a function of time requires the solution for both the eigenvectors $\mathbf{n}^j$ and the coefficients c_j in addition to the lifetimes of the states.

Consider, for example, the measurement of the lifetime of the $8\,^2P_{3/2}$ state of thallium. A calculation was performed to determine the time required for the fluorescence decay to reach within 2% of the asymptotic limit. This was done by a computer program which calculates the eigenvectors and coefficients, given the initial state and the rates for all nonforbidden (electric dipole) transitions among lower-lying states. The transition rates were taken from tables of theoretical values,[3,4] since no complete set of experimental numbers are available. This should be adequate for the present calculation, since its sole purpose is to estimate the time delay required for treating the data as a single exponential decay. These tables did not list the $n\,^2D-m\,^2F$ transitions; the effect of this exclusion is discussed later in this section.

Table II lists all fluorescence components and their calculated relative probabilities for cascade originating in the $8\,^2P_{3/2}$ state. The time evolution of the fluorescence signal depends upon the range of fluorescence wavelengths detected in the experiment. Table III(a) gives the equation for the photon rate assuming a uniform detection sensitivity within the ultraviolet spectral region (240—400 nm), and zero sensitivity elsewhere. This is a reasonable approximation of the detection system with Corning filters (no. 7-54), but without the use of a $NiSO_4$ cell. The effect of using this cell to eliminate the light at 378 nm is seen in the results printed in Table III(b); it removes the most troublesome terms in the expression, $\exp(-16.40t)$ and

TABLE II. Calculated spectrum of cascade fluorescence from the $8\,^2P_{3/2}$ initial state using transition rates from Ref. 3.

Energy (cm^{-1})	Wavelength (nm)	Probability	Transition
38746	258.1	0.1720	$8\,^2S_{1/2}-6\,^2P_{1/2}$
36118	276.9	0.0087	$6\,^2D_{3/2}-6\,^2P_{1/2}$
30953	323.1	0.1820	$8\,^2S_{1/2}-6\,^2P_{3/2}$
28407	352.0	0.0972	$6\,^2D_{5/2}-6\,^2P_{3/2}$
28325	353.0	0.0015	$6\,^2D_{3/2}-6\,^2P_{3/2}$
26478	377.7	0.2446	$7\,^2S_{1/2}-6\,^2P_{1/2}$
18685	535.2	0.2941	$7\,^2S_{1/2}-6\,^2P_{3/2}$
15263	655.2	0.4566	$8\,^2P_{3/2}-7\,^2S_{1/2}$
8684	1151.6	0.0478	$7\,^2P_{3/2}-7\,^2S_{1/2}$
7682	1301.7	0.0342	$7\,^2P_{1/2}-7\,^2S_{1/2}$
5623	1778.4	0.0102	$8\,^2P_{3/2}-6\,^2D_{3/2}$
5541	1804.8	0.0973	$8\,^2P_{3/2}-6\,^2D_{5/2}$
4586	2180.5	0.0342	$8\,^2S_{1/2}-7\,^2P_{1/2}$
3585	2789.6	0.0478	$8\,^2S_{1/2}-7\,^2P_{3/2}$
2995	3339.0	0.4359	$8\,^2P_{3/2}-8\,^2S_{1/2}$
1958	5107.3	<0.0001	$6\,^2D_{3/2}-7\,^2P_{1/2}$
1039	9626.5	0.0001	$6\,^2D_{5/2}-7\,^2P_{3/2}$
957	10451.5	<0.0001	$6\,^2D_{3/2}-7\,^2P_{3/2}$

$\exp(-21.10t)$. The time required to reach within 2% of the asymptotic limit changes from 182 ns in the former case to 96 ns in the latter. These results are also seen graphically in the semilog plots of the predicted fluorescence as a function of time (Fig. 3). Clearly, case (b) with detection of fluorescence between 240 and 350 nm is preferable.

Similar calculations were performed for all of the states investigated in order to establish the time after which the data could be fitted to the asymptotic slope. It was found that potential problems may arise in three cases: the $9\,^2P_{3/2}$, $10\,^2P_{3/2}$, and $11\,^2P_{3/2}$ initial states. The $11\,^2P_{3/2}$ state is unique in that, according to the theoretical values used, it is the only one among those considered that violates the original assumption that the initial state has a longer lifetime than all lower-lying states participating in the cascade fluorescence.. Fortunately, the troublesome term has a relatively small amplitude compared to that of the term for the initial state, contributing no more than 2% of the total when evaluated at times less than twice the lifetime of the initial state.

The other two states mentioned above pose a somewhat different problem. While they both adhere to the initial assumptions stated earlier, in each case the presence of a term with only *slightly* shorter time constant than that of the initial state means that the time required for the decay to approach the asymptote is objectionably long. This situation is illustrated in Fig. 4, where the predicted fluorescence decay from the $10\,^2P_{3/2}$ state is seen to lie considerably below the asymptote during the time period shown. However, the slope of both lines are nearly identical after one time constant of the initial state. This suggests that

TABLE III. Calculated time dependence of cascade fluorescence from the $8\,^2P_{3/2}$ state. (a) Assumes detection of fluorescence from 240 to 400 nm. (b) Assumes detection of fluorescence from 240 to 350 nm. Both the amplitude and decay constant are in units of μs^{-1}.

Amplitude	Exponential term	State responsible for exp term
	(a)	
+6.443	$\exp(-7.71t)$	$8\,^2P_{3/2}$
−0.390	$\exp(-16.40t)$	$7\,^2P_{1/2}$
−0.555	$\exp(-21.10t)$	$7\,^2P_{3/2}$
−2.899	$\exp(-47.91t)$	$8\,^2S_{1/2}$
−0.799	$\exp(-124.09t)$	$6\,^2D_{5/2}$
−1.717	$\exp(-139.40t)$	$7\,^2S_{1/2}$
−0.084	$\exp(-142.45t)$	$6\,^2D_{3/2}$
	(b)	
+3.322	$\exp(-7.71t)$	$8\,^2P_{3/2}$
−3.251	$\exp(-47.91t)$	$8\,^2S_{1/2}$
−0.071	$\exp(-142.45t)$	$6\,^2D_{3/2}$

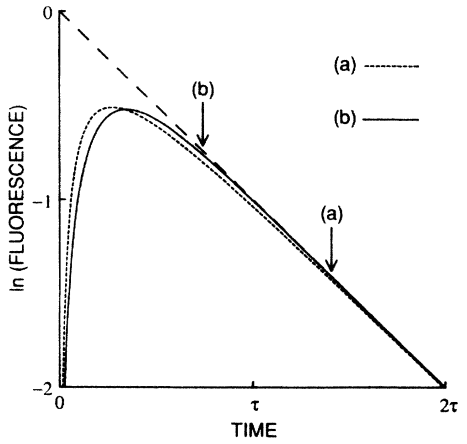

FIG. 3. Predicted cascade fluorescence from the $8\,^2P_{3/2}$ initial state, assuming light detection in the range (a) 240—400 nm and (b) 240—350 nm. The curves are normalized so as to have the same asymptotic values; the arrows indicate the points at which the respective curves approach within 2% of the asymptote.

the original criterion can be replaced with another, less stringent one. To quantify this, consider a decay consisting of just two terms: the first term representing the decay of the original state, and the second term due to a state with only a slightly shorter lifetime. (The other terms can be ignored since they all damp away quickly, as assumed in previous cases.) The fluorescence decay rate can then be written as

$$F=A_1e^{-\lambda_1 t}+A_2e^{-\lambda_2 t}$$
$$=A_1e^{-\lambda_1 t}(1+\epsilon e^{-\eta\lambda_1 t})\ . \tag{6}$$

where $\epsilon\equiv A_1/A_2<1$ and $\eta\equiv(\lambda_2-\lambda_1)/\lambda_1<1$. For example, if the first term is from the $10\,^2P_{3/2}$ initial state, then the second term would be from the next-longest-lived state, $9\,^2P_{1/2}$, giving $\eta=0.056$. If the fluorescence is detected between 240 and 350 nm, then $\epsilon=0.106$. Calculating the decay rate between two points, chosen to be at one and two lifetimes of the initial state, gives the following expression after taking the logarithm and expanding to lowest order:

$$\frac{\Delta\ln(F)}{\Delta t}\approx-\lambda_1(1+\epsilon\eta)\ . \tag{7}$$

Thus, although neither ϵ nor η is small enough to be ignored, the error introduced in the calculation of the slope in this situation is on the order of $\epsilon\eta=0.006$, which is negligible.

One remaining issue affecting these simulations is the exclusion of the ^2F states from the calculations, as mentioned earlier. The energy-level diagram of thallium in Fig. 1 shows that a ^2F state can become populated from a ^2P initial state only by decay through an intermediate ^2D state. The effect of such transitions on the lifetime measurements can be estimated qualitatively by considering the $10\,^2P_{1/2}$ initial state as an example. This is the lowest ^2P state that can populate a ^2F state, which in this case is $5\,^2F_{5/2}$. In order for the latter state to significantly affect the lifetime measurement of the initial state, two conditions are necessary: (1) The lifetime of the $5\,^2F_{5/2}$ state must be comparable to or greater than that of the initial state ($\approx$600 ns); and (2) a significant fraction of atoms must populate the $5\,^2F_{5/2}$ state by decay through the $8\,^2D_{3/2}$ state. Calculations predict that only 16% of the atoms reach the $8\,^2D_{3/2}$ state; therefore, a large fraction of *these* must decay to the $5\,^2F_{5/2}$ state in order for the latter population to be significant. This requires an $8\,^2D_{3/2}$—$5\,^2F_{5/2}$ transition rate which is fast compared to the inverse lifetime of the $8\,^2D_{3/2}$ state due to all other decay modes ($\approx$35 ns). However, the first point above requires that the decay rate *out* of the $5\,^2F_{5/2}$ state be very slow. It is rather unlikely that both conditions would be met; the oscillator strength for the $8\,^2D_{3/2}$—$5\,^2F_{5/2}$ transition would have to be larger than that for the $5\,^2F_{5/2}$—$6\,^2D_{3/2}$ (or $5\,^2F_{5/2}$—$7\,^2D_{3/2}$) transition by much more than an order of magnitude. Similar arguments apply to other initial ^2P states which lie higher than $10\,^2P_{1/2}$, although the possible transitions to the ^2F states are more numerous.

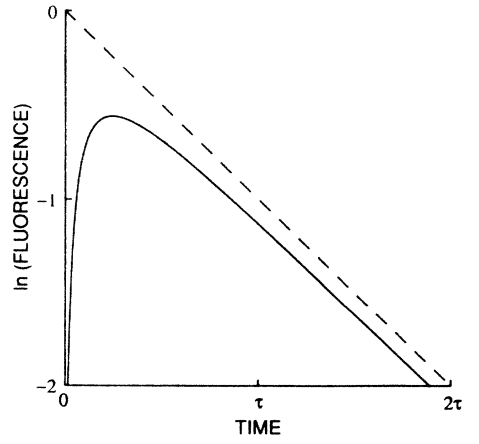

FIG. 4. Predicted cascade fluorescence from the $10\,^2P_{3/2}$ initial state. The slope of the line connecting the points at one and two lifetimes of the initial state agrees to within 0.6% of the asymptotic slope.

IV. ERRORS

Before discussing the assignment of error bars to the lifetime measurements, a brief examination of possible systematic effects is in order. Systematic errors, as opposed to random errors such as shot noise, do not decrease with increasing averaging time. They can change the average slope of decay and/or cause deviations from the predicted straight-line asymptote. Therefore, the following possible sources of error were investigated: (1) nonlinearity in the response of the PMT and measurement electronics; (2) dependence of decay rate on thallium density; and (3) dependence of decay rate on laser intensity.

The linearity check is a straightforward procedure involving measurement of a pulsed light source (such as pulsed LED) with different neutral density filters for attenuation. Two problems were identified and remedied. (1) The PMT can saturate at high peak currents at the

output stages from space-charge effects. Increasing the voltage difference across the last few dynodes of the PMT improves this significantly. (2) The offset voltage and drift of the signal averager becomes relatively important for small average signals. While offset voltage is not normally considered a contributor to nonlinearity, it is true that a nonzero base line will cause nonlinearity in the *logarithm* of the data. For fluorescence decay, this nonzero base line has the greatest effect near the end of the time sweep (where the signal is small), while random noise (shot noise and instrument noise) associated with the low signal level results in increased scatter of the data points. These problems are not as trivial to overcome as might be expected because of the wide range of photon rates encountered in the fluorescence decay. In practice then, the fitting of the logarithm of the data to a straight line is generally limited to a range of approximately twice the decay time constant. It may be possible to improve the lower limit with the use of photon-counting techniques instead of analog measurement, but this may create other problems, such as counting-rate limitations at the peak of the signal.

The dependence of decay rate on either thallium density or laser intensity might occur because of self-absorption of the fluorescence photons within the thallium beam. Although such problems are generally absent in an atomic beam, the situation may become somewhat marginal at the highest beam densities used ($N_0 \approx 10^{10}$ cm^{-3}). In order to avoid self-absorption, the following condition must be met: $N\sigma L \ll 1$, where N is the number density of absorbing atoms, σ is the cross section for absorption of the fluorescence line, and L is the average pathlength of fluorescence through the thallium (which is taken as the radius of the atomic beam, 0.35 cm). The first two parameters depend upon the particular fluorescence transition being considered. With only radiative damping present, the cross section for absorption can be taken as

$$\sigma \approx \sigma_0/\Gamma = 2\pi r_0 c f/\Gamma \ , \tag{8}$$

where σ_0 is the integrated absorption cross section for the transition, Γ is the width of the transition, r_0 is the classical radius of the electron, and f is the absorption oscillator strength.[8] The estimation of N is not quite so straightforward. Of course, as an upper bound it can be taken to be N_0, the total number density of thallium atoms, but a much better estimate can be made that takes into account the average probability of an atom being in a particular state. If we denote as $\bar{n}_i$ the population of the ith state averaged over one lifetime of the initial state, then from Eq. (4) we obtain

$$\bar{n}_i = \sum_j c_j (\mathbf{n}^j)_i (1 - e^{-t/\tau_j}) \tau_j / \tau_N \ . \tag{9}$$

Using this estimate of $N \approx \bar{n}_i N_0$, we are prepared to check for the highest value of $N\sigma L$ among all the transitions for each initial condition. Calculations show that in each of the eight initial states considered, it is the n^2P–n^2S transition that has the greatest chance of self-absorption. Table IV shows that $N\sigma L$ for this transition behaves as follows: It is larger for the $j=\frac{3}{2}$ initial state than for the $j=\frac{1}{2}$ state, and it increases steadily with principal quantum number n. This is consistent with the longer lifetimes of the higher nP states.

Of the measurements performed, the one most likely to be susceptible to self-absorption is the $11\,^2P_{3/2}$ state, with a value of $N\sigma L = 0.377$ for the transition indicated. Therefore, the measurement of this state was repeated to check for a possible density dependence in the result. The lifetime was found to be independent of thallium density over more than an order of magnitude variation. (No dependence on the spot size of the laser beam was found either.) This is not surprising, though, because the previous calculation assumes that all of the thallium atoms within the beam are excited by the laser. This assumption errs in two ways. (1) When the laser beam is focused, the width of the interaction region is determined by the width of the laser at its beam waist, not by the width of the thallium beam. Generally, the pathlength of the fluorescence through the region of excited atoms is shorter than the atomic beam radius by more than an order of magnitude. (2) If the laser beam remains unfocused so as to illuminate thallium atoms over the entire width of the atomic beam, then the laser intensity drops to a level where the proba-

TABLE IV. Estimate of self trapping in $n\,^2P$–$n\,^2S$ transitions. These are based on absorption f values from Anderson (Ref. 4), assuming a thallium number density of 10^{10} atoms/cm^3 and a pathlength $L=0.35$ cm.

Initial state	Lower state	Av. population in lower state	σ (10^{-9} cm^2)	$N\sigma L$
$7\,^2P_{1/2}$	$7\,^2S_{1/2}$	0.0686	0.148	0.036
$7\,^2P_{3/2}$	$7\,^2S_{1/2}$	0.0858	0.288	0.086
$8\,^2P_{1/2}$	$8\,^2S_{1/2}$	0.0325	0.574	0.065
$8\,^2P_{3/2}$	$8\,^2S_{1/2}$	0.0394	1.074	0.148
$9\,^2P_{1/2}$	$9\,^2S_{1/2}$	0.0191	1.565	0.105
$9\,^2P_{3/2}$	$9\,^2S_{1/2}$	0.0226	2.834	0.224
$10\,^2P_{1/2}$	$10\,^2S_{1/2}$	0.0117	3.444	0.141
$10\,^2P_{3/2}$	$10\,^2S_{1/2}$	0.0142	6.239	0.310
$11\,^2P_{1/2}$	$11\,^2S_{1/2}$	0.0084	6.486	0.191
$11\,^2P_{3/2}$	$11\,^2S_{1/2}$	0.0096	11.228	0.377

bility of two-photon absorption is much less than one. Either condition (1) or (2) above (or a combination thereof) is sufficient to drastically reduce the amount of self-absorption compared to that calculated in Table IV.

In addition to systematic errors, random errors attributable to statistical fluctuations in the fluorescence signal lead to uncertainties in the lifetimes. One way to estimate this uncertainty is by examining how well the logarithm of the data fits a straight line. (This fit begins at an initial time T_0 which is determined for each state as explained in Sec. III.) The uncertainty in the slope as indicated by the sum of squares of the deviations of the data points from the straight line is usually quite good—often less than 1%. However, the repeatability of the slope for duplicate data runs is not always as favorable. Furthermore, in spite of every effort to account for and eliminate systematic effects as described previously, some results display residual variations in the decay signal that are not purely random. Also, an uncertainty in the instrument zero is seen in the appearance of small nonzero values for the initial data points of the curve, which are sampled before the onset of the laser pulse.

In an attempt to include these uncertainties in the error bar for the lifetime values, each data run is subjected to four analyses. (1) The data is fit to a straight line over two separate time ranges— T_0 to $T_0+\tau$ (τ is nominally one lifetime), and $T_0+\tau$ to $T_0+2\tau$. Any slight curvature in the logarithm of the decay causes somewhat different results for these two slopes. (2) Each of these two fits is repeated with the base line of the data shifted so that the initial points are zero. By combining these four lifetime values of each data set together for all runs of a particular state, a mean value of the lifetime is computed along with a standard deviation. From the standard deviation is computed the deviation of the mean, which would normally be the expected uncertainty in the mean value due to statistical fluctuations. However, it may be more prudent to use the larger number given by the standard deviation of the set of measurements as an indicator of the possible range of systematic errors in the result. Both values are reported for comparison.

V. RESULTS AND DISCUSSION

Table V shows our measured lifetimes of the $n\,^2P_{1/2,3/2}$ states of thallium for $n=7-11$. Other columns in this table give statistical deviations for these measurements, data from other sources, and values from semiempirical calculations.

Examination of the first four columns reveals that the deviations of the means for all the states studied are less than 2%; however, keeping in mind the approximations of Sec. III as well as the discussion above, these uncertainties should not be taken too seriously. The more conservative error estimate is from the standard deviation, which is closer to 5% in most cases. The numbers shown for the $7\,^2P$ states reflect the current measurements taken with the new instruments. The values agree with our previous numbers to within the combined errors of the measurements.

The only other known experimental results for lifetimes in this series are the four values found in column 5 of Table V. The lifetime of the $9\,^2P_{3/2}$ state is from Shimon and Erdevdi,[9] and the other three ($8\,^2P_{3/2}$, $7\,^2P_{1/2,3/2}$) are from Hunter, Commins, and Roesch.[5] The value of the former, 16.0 ns, differs from both our experimental result and the predicted values by more than an order of magnitude. It has been suggested[3] that this low value may be due to a misidentification of spectral lines studied in the experiment. Certainly, some mistake of this significance would be needed to account for the enormous discrepancy with the theoretical and other experimental values. The results of Hunter, Commins, and Roesch[5] show much better agreement with our present measurements. Their values for the lifetimes of the $7\,^2P_{1/2}$ and $8\,^2P_{3/2}$ states

TABLE V. Comparison of lifetimes (in ns) from the present measurements with other data and semiempirical calculations. Included with the present results are the standard deviation and the deviation of the mean for our measurements.

Initial state	Current result	σ	σ of mean	Other expt.	Calc. Ref. 3	Calc. Ref. 4
$7\,^2P_{1/2}$	63.1	1.7	0.2	58.5[a]	61.0	57.7
$7\,^2P_{3/2}$	48.6	1.3	0.2	42.2[a]	47.4	45.1
$8\,^2P_{1/2}$	184.1	4.4	1.3		184.5	168.3
$8\,^2P_{3/2}$	127.7	4.9	1.2	108.7[a]	129.7	116.6
$9\,^2P_{1/2}$	391.1	21.8	5.8		380.4	345.9
$9\,^2P_{3/2}$	273.6	13.5	4.3	16.0[b]	267.0[c]	219.9
$10\,^2P_{1/2}$	656.8	14.5	3.6			613.4
$10\,^2P_{3/2}$	480.8	31.6	7.1			411.9
$11\,^2P_{1/2}$	991.1	50.8	12.7			977.0
$11\,^2P_{3/2}$	725.5	28.8	9.1			553.6

[a]Reference 5.

[b]Reference 9.

[c]This value from Ref. 3 is not consistent with that obtained by inverting the sum of the individual decay rates given in the same reference. Dr. Norcross has kindly informed us that the decay rate for the $9\,^2P_{3/2}-7\,^2D_{3/2}$ transition is misprinted in Ref. 3; it is too high by precisely an order of magnitude. The lifetime of the $9\,^2P_{3/2}$ state is nevertheless correctly given in Ref. 3.

differ from ours by approximately the combined uncertainties of the measurements (taking just 1σ as our error). The measurements of the lifetime of the $7\,^2P_{3/2}$ state, which do not agree as well, differ by about twice the combined uncertainties. We have noted that all of their lifetime measurements are shorter than our own. Their paper does refer to problems of lifetime shortening found at higher densities, and the need to correct for the effect of stimulated emission on the lifetime.[5] On the other hand, the possibility has recently been raised[10] that these lifetimes are overestimated by 13% because of a neglected term in the analysis, although the original authors claim that this contributes less than 1% error.[11] However, any attempt to correct for such an error would only increase, not decrease the discrepancy with our results.

Perhaps the major benefit of the measurement of lifetimes by monitoring fluorescence decay is the inherent simplicity of the experiment. It is a direct lifetime measurement; it does not require determination of other experimental or atomic parameters. This statement may seem to contradict the impression given by the calculations of Sec. III, which contains an analysis of the decay from all states involved in the cascade. However, this information is sought only to establish the independence of the relevant portion of the decay curve from a detailed knowledge of the other transition rates within the atom; it is not a calculation performed for direct inclusion in the final lifetime value, nor is it used as a correction to the values analyzed. Thus, because the goal is only to establish independence of the need for such correction, it is generally true that errors in the values used for the computations of Sec. III should affect our results only weakly, if at all. This is why our use of somewhat uncertain theoretical numbers in the simulations should not be cause for undue concern. Nevertheless, it might be desirable to perform similar experiments which detect only the fluorescence originating from the initial state, such as that due to the $n\,^2P$–$7\,^2S_{1/2}$ transition, thus avoiding completely the need for simulations. For instance, the $11\,^2P_{1/2}$–$7\,^2S_{1/2}$ transition yields fluorescence at 489.2 nm with approximately 30% efficiency. It should not be difficult to isolate this line from other spectral emissions, although problems may arise because this line is longer in wavelength than the excitation light, and it lies in the visible spectrum where the background intensity is considerably higher.

Comparison of our results with the theoretical calculations in the last two columns of Table V allows some conclusions to be drawn about the latter. Agreement between our values and those predicted by Bardsley and Norcross[3] is quite good, with an average discrepancy of about 2%. Unfortunately, their published tables do not include the calculations for the higher $n\,^2P$ states ($n \geq 10$); our comparison for these cases is necessarily restricted to the calculations by Anderson.[4] These theoretical lifetimes do not agree as well as those in the first comparison, and they are consistently shorter than our measured lifetimes. However, it is interesting to note that these values of Anderson are also lower than those of Bardsley and Norcross for the cases where $n < 10$. This seems to lend further credence to claims by the latter that their inclusion of core-polarization effects leads to greater accuracy than previous calculations which neglected this effect.

Our results also show that one of the concerns raised in Sec. III proved to be unnecessary. The experimental value for the lifetime of the $11\,^2P_{3/2}$ state is 725 ns; it is longer than that of all lower-lying states which contribute to the fluorescence, including the $10\,^2P_{1/2}$ state with a measured lifetime of 656 ns. The theoretical numbers of Anderson predict a shorter lifetime for the $11\,^2P_{1/2}$ state (553 ns) than for the $10\,^2P_{3/2}$ state (613 ns). This difference between theory and measurement exemplifies the importance of experimentally testing the various models used in calculating wave functions and transition matrix elements. One current application of such calculations is in the interpretation of parity nonconservation experiments[12] (PNC) which have been performed in thallium and other similar elements. Although these calculations do not generally employ the lifetimes of the states directly, these lifetime measurements provide a useful check of the models used in the PNC calculations. Our experimental results for the $n\,^2P$ states of thallium may prove useful in this context, along with previous measurements involving other states of thallium.

ACKNOWLEDGMENT

One of the authors (J.V.J.) has included this work as part of a doctoral dissertation at the University of Michigan.

[1]J. V. James, C. C. Wang, and C. Guo, Phys. Rev. A **32**, 643 (1985).

[2]P. F. Gruzdez, Opt. Spectrosc. **20**, 209 (1966); J. Miqdalek, Can. J. Phys. **54**, 118 (1976); D. V. Neuffer and E. D. Commins, Phys. Rev. A **16**, 844 (1977); P. F. Gruzdev and N. V. Afanaseva, Opt. Spectrosc. **44**, 614 (1978).

[3]J. N. Bardsley and D. W. Norcross, J. Quant. Spectrosc. Radiat. Transfer **23**, 575 (1980).

[4]E. M. Anderson, E. K. Anderson, and V. F. Trusov, Opt. Spectrosc. **22**, 471 (1967).

[5]L. Hunter, E. Commins, and L. Roesch, Phys. Rev. A **25**, 885 (1982).

[6]The lifetime measurements from Ref. 5 were inadvertently overlooked in our previous paper.

[7]C. E. Moore, *Atomic Energy Levels*, Natl. Bur. Stand. (U.S.) Circ. No. 35 (U.S. GPO, Washington, D.C., 1971), Vol. 3, pp. 202 and 203.

[8]A. Corney, *Atomic and Laser Spectroscopy* (Oxford University Press, Oxford, 1977), p. 285.

[9]L. L. Shimon and N. M. Erdevdi, Opt. Spectrosk. **42**, 241 (1977) [Opt. Spectrosc. (USSR) **42**, 137 (1977)].

[10]L. Hunter, G. M. Watson, D. S. Weiss, A. G. Zajonc, Phys. Rev. A **31**, 2268 (1985).

[11]L. Hunter (private communication).

[12]P. S. Drell and E. D. Commins, Phys. Rev. Lett. **53**, 968 (1984); W. R. Johnson, D. S. Guo, M. Idrees, J. Sapirstein, Phys. Rev. A **32**, 2093 (1985).